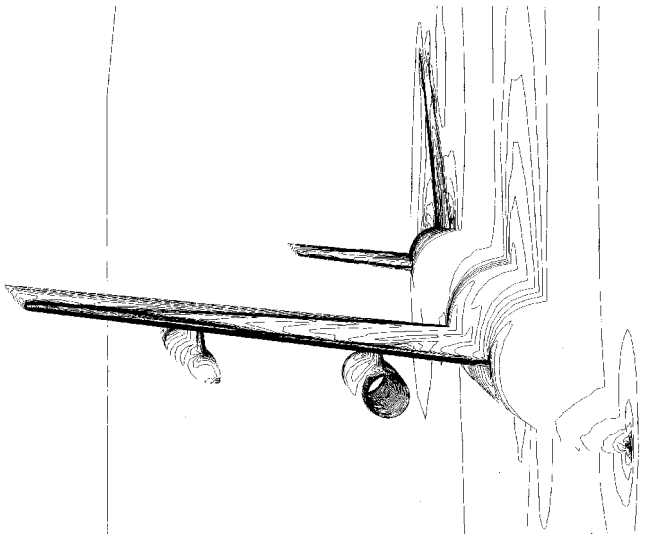

Fig. 4 C_p contours at 0.05 intervals on the aircraft configuration at M_∞ = 0.9 and angle of attack = 4 deg.

ment of this mesh. On the contrary, the upwind scheme can capture the vortex accurately. The residual is reduced by 3.5 orders of magnitude in 800 iterations. Note that this condition is also computed by using a total variation diminishing scheme in a multiblock grid with 89,012 nodes.[11] The computed results are compared with wind-tunnel results in Fig. 3. The lambda shock on the upper wing and the small leading-edge vortex are well captured. The wingtip flow is subject to strong viscous effect and cannot be resolved by using the Euler equations. Overall, the computed result is within what one would expect from a good Euler simulation.

The wing–body configuration is not complicated enough to demonstrate the autostretching method. To show this mesh generator does work, vertical and horizontal tails, pylon-mounted flow-through engine nacelles, and stores are added to the wing–body configuration without considering any aircraft design rules. To generate the volume mesh, the stretching ratio used is 1.15. A total of 119,797 tetrahedra and 23,139 nodes are generated with 4208 nodes on the surface. The flow condition is Mach number 0.9 and an angle of attack of 4 deg. The C_p contours are shown in Fig. 4. Because there is no experimental data and the mesh is not fine enough, discussion on the flowfield is therefore not attempted.

References

[1]Lin, H.-C., "An Auto-Stretching Method for Fast Generation of Unstructured Grids for Complex Configurations," *Proceedings of the 17th National Conference on Theoretical and Applied Mechanics* (Taipei, Taiwan, ROC), Chinese Society of Theoretical and Applied Mechanics, 1993, pp. 43–50.

[2]Peraire, J., Vahdati, M., Morgan, K., and Zienkiewicz, O. C., "Adaptive Remeshing for Compressible Flow Computations," *Journal of Compuational Physics*, Vol. 72, No. 4, 1987, pp. 449–466.

[3]Jameson, A., Baker, T. J., and Weatherill, N. P., "Calculation of Inviscid Transonic Flow over a Complete Aircraft," AIAA Paper 86-0103, Jan. 1986.

[4]Frink, N. T., Parikh, P., and Pirzadeh, S., "A Fast Upwind Solver for the Euler Equations on Three-Dimensional Unstructured Meshes," AIAA Paper 91-0102, Jan. 1991.

[5]Thareja, R. R., Stewart, J. R., Hassan, O., Morgan K., and Peraire, J., "A Point Implicit Unstructured Grid Solver for the Euler and Navier-Stokes Equations," *International Journal for Numerical Methods in Fluids*, Vol. 9, No. 5, 1989, pp. 405–425.

[6]Loving, D. L., and Estabrooks, B. B., "Transonic-Wing Investigation in the Langley 8-Foot High-Speed Tunnel at High Subsonic Mach Numbers and at Mach Number of 1.2—Analysis of Pressure Distribution of Wing-Fuselage Configuration Having a Wing of 45 Sweepback, Aspect Ratio 4, Taper Ratio 0.6, and NACA 65A006 Airfoil Section," NACA RM L51F07, May 1951.

[7]Bonet, J., and Peraire, J., "An Alternate Digital Tree Algorithm for Geometric Search and Intersection Problems," *International Journal for Numerical Methods in Engineering*, Vol. 31, No. 1, 1991, pp. 1–17.

[8]Peraire, J., Morgan, K., and Peiro, J., "Unstructured Mesh Methods for CFD," von Kármán Inst. for Fluid Dynamics Lecture Series 1990-06, Brussel, Belgium, 1990.

[9]Löhner, R. L., "Some Useful Data Structures for the Generation of Unstructured Grids," *Communications in Applied Numerical Methods*, Vol. 4, No. 2, 1988, pp. 123–135.

[10]Wey, T. C., and Li, C. P., "Numerical Simulation of Shuttle Ascent Transonic Flow Using an Unstructured-Grid Approach," *Computers and Structure*, Vol. 39, No. 1/2, 1991, pp. 21–46.

[11]Wang, C.-J., and Chakravarthy, S. R., "Transonic Euler Calculations of a Wing-Body Configuration Using a High-Accuracy TVD Scheme," AIAA Paper 88-2547, July 1988.

Effects of Asymmetric Leading-Edge Flap Deflection on Delta Wings in Roll

Carlos Ize* and Andrew S. Arena Jr.†
Oklahoma State University, Stillwater, Oklahoma 74078

Introduction

A STUDY has been conducted to explore the effects of leading-edge vortex flaps on the rolling moment of delta wings over a wide angle of attack range. Leading-edge flaps with a conical planform were tested on flat plate delta wings of 65- and 80-deg sweep angles. The effects of antisymmetric deflection was investigated to assess the effectiveness of the flaps for this task over a wide operating envelope. Data are collected over a wide range of angles of attack that includes attached and separated flow conditions.

Experimental Setup

Experiments were conducted in the indraft wind tunnel at Oklahoma State University. The test section has a 0.93 × 0.93 m cross section and a length of 2.81 m. Throughout the study, a tunnel dynamic pressure of 244 Pa was maintained. The conditions were the same for all experiments.

The delta wing models used in the experiments had 65- and 80-deg sweep angles and are shown in Figs. 1a and 1b. Both were made out of aluminum, and the planform area was equal to 428 cm^2 for both wings. Each leading edge was beveled 45 deg and the flaps were such that at each chord station the flap span was 20% of the local span, yielding a conical geometry.

The torque sensor was of cruciform type, and was used to measure rolling moment C_l. The torque sensor was built to be a temperature-compensated Wheatstone bridge. The wing and the sensor were sting mounted in a base to minimize downstream interference effects, shown in Fig. 1c.

The rolling moment for the wings with flaps deflected was measured at angles of attack from $\alpha = -2$ to $+32$ deg in 2-deg increments. The flaps were set at $\delta = 25$ deg antisymmetrically, relative to the wing, with the port flap being downward and the starboard flap upward.

Received Sept. 10, 1997; revision received June 9, 1998; accepted for publication June 24, 1998.

*Graduate Research Assistant, School of Mechanical and Aerospace Engineering. Student Member AIAA.

†Assistant Professor, School of Mechanical and Aerospace Engineering. Senior Member AIAA.

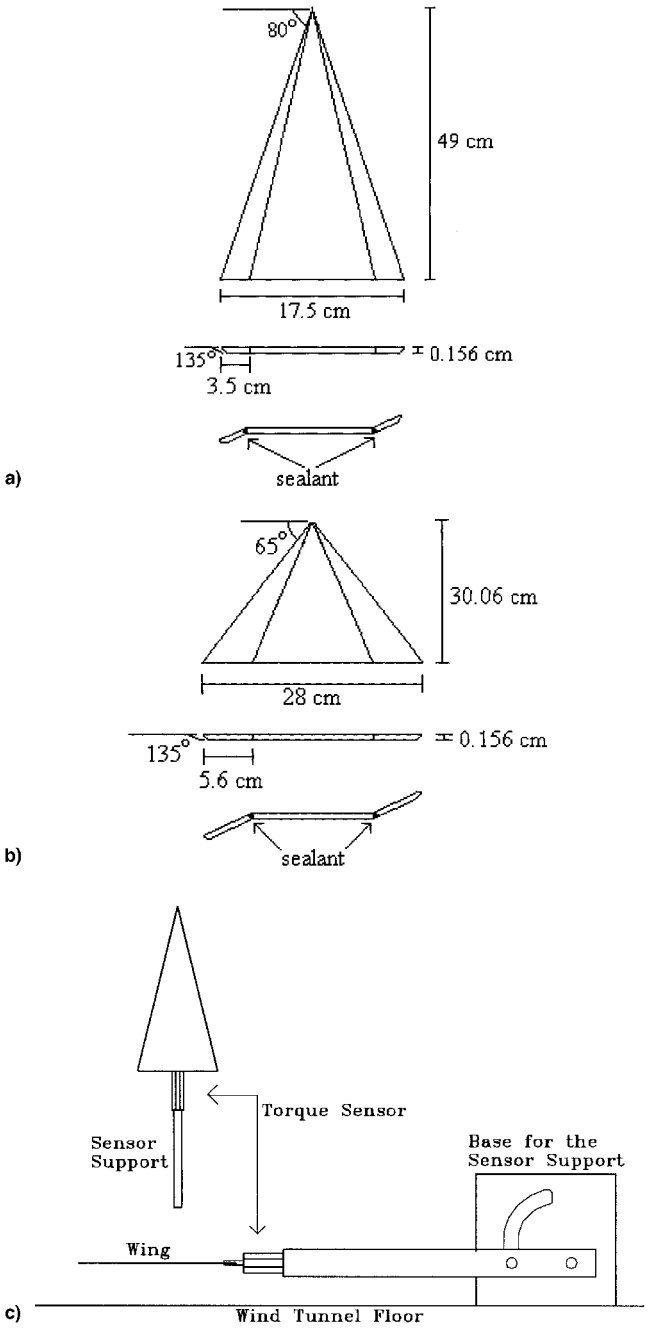

Fig. 1 a) 80-deg sweep angle delta wing with 20% conical flap; b) 65-deg sweep angle delta wing, with 20% conical flap; and c) sting mount and sensor schematic (not in scale).

Calibration was accomplished using known weights at a given moment arm before and after each experiment. Normal and lateral force coupling were assessed and found to be unmeasurable. The maximum uncertainty on the measurement of the rolling moment was 4%. The experiments were made for several roll angles and angles of attack for the plane wings.

Computer Code

The computational analysis for this study was performed using a modified model developed by Arena and Nelson.[1] The model assumes conical flow over a slender wing, which implies that all cross sections of the flow are consistent, varying only by a linear scaling factor. The use of the code for this study was limited to providing additional insight into the observed experimental data for angles of attack where vortices are present.

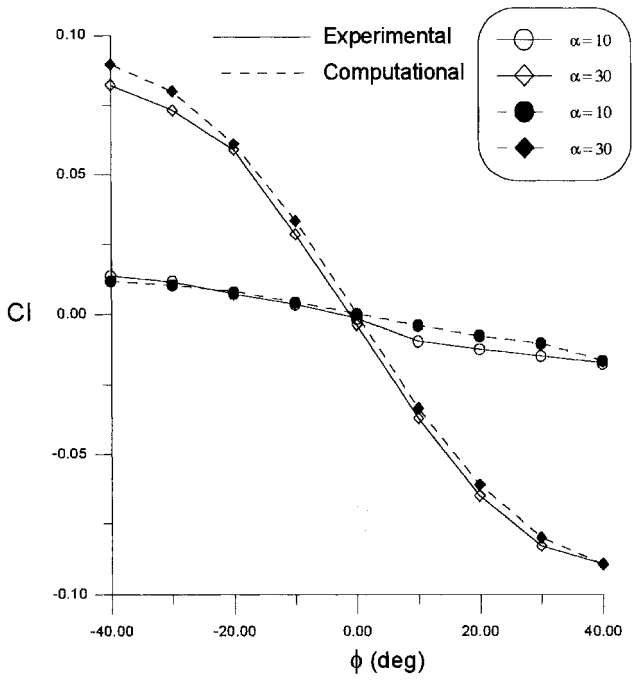

Fig. 2 Roll moment coefficient vs roll angle ϕ for different angles of attack, for the 80-deg sweep angle delta wing.

The code was extensively used by Roberts and Arena.[2] Static and dynamic tests were conducted and compared with experimental data. Further discussion of validation runs may be obtained in Ref. 1.

The code was used previously by Ize and Arena[3] to study the quasisteady effects on a delta wing. The program was then modified, allowing the use of the leading edges of the wing to model vortex flaps. The vortex flaps modify the characteristics of the separation and, therefore, the primary vortex position and strength. Flap deflection angles are calculated during the coupled solution, such that any practical deflection strategy may be assessed.

For the 80-deg wing with no flap deflection, the moment coefficient is shown in Fig. 2, comparing the experimental and computational data. Good agreement is observed between the experiment and computed results. The code uses potential flow to model the leading-edge vortices over the wing. Therefore, for the 80-deg wing at small angles of attack, the vortices are not formed, and the assumptions in the code are not valid. For angles of attack higher than 32 deg, vortex breakdown starts to appear on the wing, which is not modeled in the code. Therefore, the use of the code was limited to angles of attack between approximately 12 and 30 deg, for the 80-deg wing.

For a 25-deg asymmetric flap deflection, the comparison between experimental and computational models, shown in Fig. 3a, is also good. The code predicts the left vortex becomes stronger than the right vortex, generating a rolling moment to the right, as shown in Fig. 3b.

Results

Flap Deflection

The effect of a 25-deg antisymmetric flap deflection on the 80-deg wing and on the 65-deg wing is shown in Fig. 4. The plot in Fig. 4a, shows that for the 80-deg delta wing, the rolling moment coefficient increases for angles of attack higher than 5 deg. If the angle of attack is approximately 5 deg, all control effectiveness is lost, and for angles of attack smaller than 5 deg, an interesting phenomenon may be seen in which antisymmetric flap deflection produces a moment in the positive direction. A similar behavior was observed for the 65-deg wing; however, the reversal occurs at a larger angle of attack, as shown in Fig. 4b. The figure indicates that above an angle

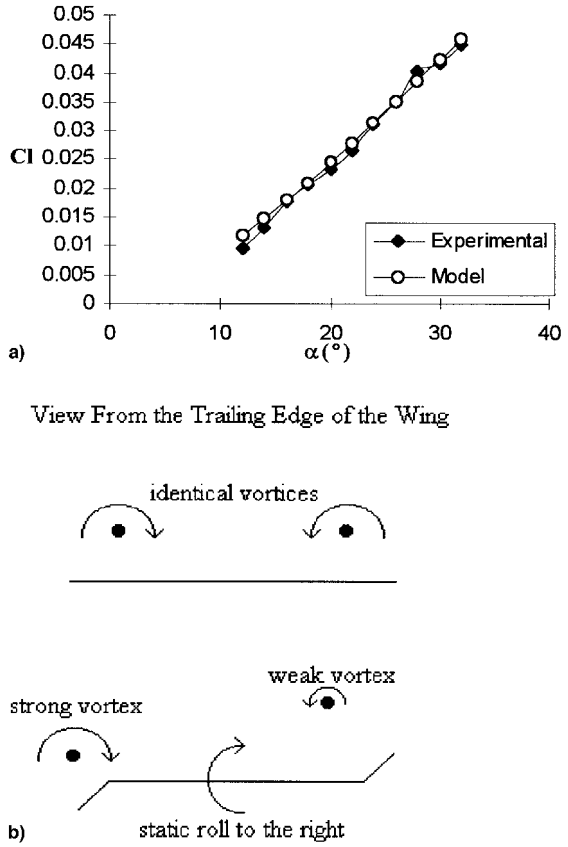

Fig. 3 a) Comparison between experiment and computer model for 25-deg asymmetric flap deflection, on the 80-deg wing; and b) delta wing without and with flap deflection.

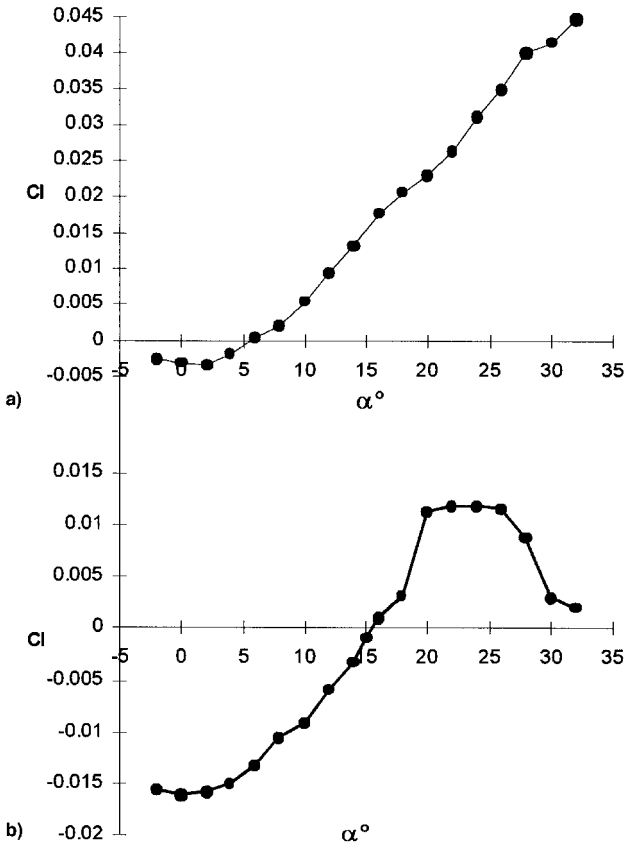

Fig. 4 Effect of asymmetric flap deflection on C_l for different angles of attack: a) 80- and b) 65-deg wing.

of attack of approximately 15 deg, an increase in angle of attack increases control effectiveness up to $\alpha = 20$ deg, where effectiveness is constant, and above 25-deg angle of attack, the effectiveness is reduced. At an angle of attack of approximately 32 deg, the control effectiveness is essentially zero. It is speculated that this decrease in control effectiveness is because of the effects of vortex breakdown that appears on the 65-deg wing for angles of attack greater than 20 deg.[4]

Analysis of Results

There are several different phenomena observed for the delta wings when leading-edge flaps are deflected asymmetrically. First, effectiveness of the flaps appear to be a strong function of wing sweep angle and angle of attack. Flap effectiveness for the 80-deg wing increases with α and is very good at large angles of attack. Conversely, the effectiveness of the flaps on the 65-deg wing is degraded beyond approximately 26 deg; however, effectiveness is best at the lowest angles of attack, although in the opposite direction.

Another significant observation for both wings is the reversal of roll moment with angle of attack. In each case there is a positive angle of attack for which control effectiveness is zero. Roll moment behavior caused by asymmetric flap deflection is in the opposite direction for angles of attack on either side of this zero effectiveness point.

An explanation for this behavior may be understood by considering both longitudinal and lateral flow effects. At low angles of attack as the leading edge flap is deflected upward, the local angle of attack is increased, as shown in Fig. 5a, and vice versa on the opposite flap. This will create a roll moment toward the *downward* deflected flap. Conversely at larger angles of attack, the crossflow becomes dominant because of the leading-edge vortex formation. A downward deflected flap results in a stronger vortex closer to the wing as observed in Fig. 5b, and as predicted by the computer model shown in Figs. 3a and 3b. The result is a roll moment in the direction of the *upward* flap. This behavior would then be further modified by the appearance of vortex breakdown, which is suspect in creating the decrease in effectiveness beyond 26-deg angle of attack, for the 65-deg wing.

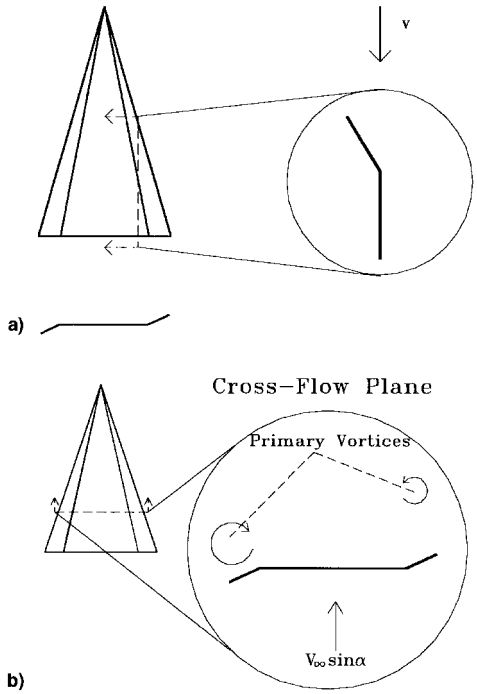

Fig. 5 a) Effect of flap deflection at low angles of attack and b) effect of flap deflection at high angles of attack.

Conclusions

The goal of the present study was to assess the roles of asymmetric leading-edge flap deflections on delta wings over a wide range of angle of attack, including attached and separated flow regimes. Experimental and computational modeling data were collected for both 80- and 65-deg delta wings with 20% conical flaps.

A significant observation was that both wings exhibited a reversal in control effectiveness at an angle of attack dependent on sweep angle. The reversal behavior may result from the relative strengths of the longitudinal and crossflow effects.

References

[1]Arena, A. S, Jr., and Nelson, R. C., "A Discrete Vortex Model for Predicting Wing Rock of Slender Wings," AIAA Paper 92-4497, Aug. 1992.

[2]Roberts, S. D., and Arena, A. S., Jr., "An Inviscid Model for Evaluating Wing Rock Suppression Methodologies," AIAA Paper 94-0808, Jan. 1994.

[3]Ize, C., and Arena, A. S., Jr., "Spanwise Camber and Quasi-Steady Effects During Wing Rock," AIAA Paper 97-0325, Jan. 1997.

[4]Wentz, W. H., Jr., and Kohlman, D. L., "Vortex Breakdown on Slender Sharp-Edged Wings," *Journal of Aircraft*, Vol. 8, No. 3, 1971, pp. 156–161.

Identifying Aerial Bomb's Aerodynamic Drag Coefficient Curve Using Optimal Dynamic Fitting Method

Yangquan Chen*
National University of Singapore, Singapore 119260, Singapore
Changyun Wen†
Nanyang Technological University, Singapore 639798, Singapore
and
Mingxuan Sun‡
Xi'an Institute of Technology, 710032 Xi'an, People's Republic of China

Introduction

TO increase the bombing accuracy of aerial bombs from aircrafts, the use of the aerial bomb's drag coefficient curve plays a crucial role. There are two ways to obtain such a curve. The first is by wind-tunnel testing. The second is by theoretical numerical prediction. As, when bombing, the mechanism of the interference air flowfield between the aircraft and the aerial bomb is not yet clear at the present time, the drag coefficient curve obtained from either wind-tunnel measurements or theoretical numerical prediction under the free airflow condition cannot be applied directly. The curve reduced from real flight testing data is obviously advantageous in practical applications. Many efforts have been made in identifying aerodynamic properties of real or full-scale flying vehicles from flight-testing data.[1–5] Most existing literature only emphasizes the aerodynamic coefficient extraction by parameter identification. Directly identifying aerial bomb's aerodynamic coefficient curve, especially the Mach history, has not yet been discussed. Also, it has been argued that the time history of the aerodynamic property is not preferred to be extracted directly.[6] In fact, from the intrinsic characteristic of aerodynamics, the aerodynamic property curves (Mach history) are generally invariant in different flight tests if the angle of attack along the trajectory is small, and can be regarded as deterministic control profiles from the control point of view. The aerodynamic property curve identification can then be considered as an optimal tracking control problem (OTCP), where the aerodynamic property curve is the control profile and the flight testing data are the desired trajectories to be optimally tracked. This identified curve is called aerial bomb's optimal fitting drag coefficient curve $C_{df}(M)$. This optimal control problem can be solved by nonlinear programming via a parameterization of the control function,§ but only the time history of the control can be considered. In this Note, the control profile $C_{df}(M)$, rather than $C_{df}(t)$, is directly considered by an optimal dynamic fitting scheme. In the scheme, $C_{df}(M)$ is parameterized by cubic splines with a deficiency number of 2. Thus, the first-order derivative of $C_{df}(M)$ is guaranteed to be continuous. The standard Newton–Raphson iteration is applied. To reduce the computational cost, an idea of quasi-Newton–Raphson iteration is proposed. This can also achieve the second-order convergence that cuts the computing cost by half, even if the first-order gradient alone is used. In addition, the initial system states for flight testing, which may be uncertain or inaccurate, can be easily identified or corrected together with the optimal dynamic fitting procedure. As real flight testing was conducted to obtain the data for aerodynamic curve identification, we believe that the obtained results are rather convincing in applications including the verification and improvement of design objectives, validation of computational aerodynamic property prediction codes, etc.

Problem Formulation

To simplify our discussion, a three-degree-of-freedom point mass ballistic model is used. Suppose at time t, the aerial bomb's position in the earth coordinate system (ECS) is $[x(t), y(t), z(t)]^T$, and its relative velocity vector $\boldsymbol{u}$ w.r.t. ECS is $[u_x(t), u_y(t), u_z(t)]^T$. We have

$$\begin{aligned}
\dot{u}_x &= f_1[\boldsymbol{X}(t), C_{df}(M)] = -\rho s V(u_x - w_x)C_{df}(M)/2m \\
\dot{u}_y &= f_2[\boldsymbol{X}(t), C_{df}(M)] = -\rho s V u_y C_{df}(M)/2m - g \\
\dot{u}_z &= f_3[\boldsymbol{X}(t), C_{df}(M)] = -\rho s V(u_z - w_z)C_{df}(M)/2m \\
\dot{x} &= f_4[\boldsymbol{X}(t), C_{df}(M)] = u_x \\
\dot{y} &= f_5[\boldsymbol{X}(t), C_{df}(M)] = u_y \\
\dot{z} &= f_6[\boldsymbol{X}(t), C_{df}(M)] = u_z
\end{aligned} \tag{1}$$

where $\boldsymbol{X}(t) = [x, y, z, u_x, u_y, u_z]^T$, which is the state vector of system (1); g is the gravitational acceleration; w_x, w_z are wind components in ECS; V is the aerial bomb's relative velocity w.r.t. wind and given by

$$V = \sqrt{(u_x - w_x)^2 + u_y^2 + (u_z - w_z)^2} \tag{2}$$

ρ is the air density; $s = \pi d^2/4$, which is the reference area of aerial bomb; d is the aerial bomb's diameter; and m is the mass of the aerial bomb. $C_{df}(M)$ is the fitting drag coefficient curve w.r.t. the trajectory model (1), which is regarded as a control profile to be solved. M denotes the Mach number and is given

Received Sept. 9, 1997; revision received April 17, 1998; accepted for publication July 5, 1998.

*Professional Officer, Department of Electrical Engineering, 10 Kent Ridge Crescent. E-mail: yqchen@shuya.ml.org.

†Senior Lecturer, School of Electrical and Electronic Engineering, Nanyang Avenue, E-mail: ecywen@ntu.edu.sg.

‡Associate Professor, Department of Electrical Engineering.

§Schwartz, A. L., E. Polak, and Y. Chen. "RIOTS_95 (Recursive Integration Optimal Trajectory Solver)—A Matlab Toolbox for Solving Optimal Control Problems," Version 1.0 for Windows. URL: http://turnpike.net/~RIOTS, 1997.